NASA TECHNICAL NOTE

NASA TN D-4583

C. 1

NASA TN D-4583



# A HIGH ENTHALPY PLASMA GENERATOR FOR ENTRY HEATING SIMULATION

*by Charles E. Shepard, Donald M. Ketner, and John W. Vorreiter*

*Ames Research Center*
*Moffett Field, Calif.*

NATIONAL AERONAUTICS AND SPACE ADMINISTRATION • WASHINGTON, D. C. • MAY 1968

# A HIGH ENTHALPY PLASMA GENERATOR FOR ENTRY HEATING SIMULATION

By Charles E. Shepard, Donald M. Ketner, and John W. Vorreiter

Ames Research Center
Moffett Field, Calif.

NATIONAL AERONAUTICS AND SPACE ADMINISTRATION

For sale by the Clearinghouse for Federal Scientific and Technical Information
Springfield, Virginia 22151 – CFSTI price $3.00

# A HIGH ENTHALPY PLASMA GENERATOR FOR ENTRY HEATING SIMULATION*

By Charles E. Shepard, Donald M. Ketner,
and John W. Vorreiter

Ames Research Center

## SUMMARY

The Constricted-Arc Supersonic Jet, capable of center-line enthalpies in excess of $3\times10^8$ joules/kg (130,000 Btu/lb), has a variety of applications, the most important probably being the simulation of entry heating from interplanetary missions. Within a Constricted-Arc Supersonic Jet apparatus, a supersonic nozzle with an elongated throat, or arc constrictor, a direct-current arc and a longitudinal flow of gas are maintained. The working fluid, which may be air or any other gas, is heated as it passes near the arc, becomes electrically conductive and eventually becomes a part of the arc core. The arc core temperature is maintained by current flow while the gas passes through the supersonic nozzle into the test section.

Ames Research Center has built and tested several configurations of the Constricted-Arc Supersonic Jet, the largest of which operates at a power input of 5 MW with an efficiency of about 50 percent. The performance of these devices can be described by defining an effective flight velocity and altitude. At present, total enthalpies and impact pressures corresponding to flight at 10 km/s at 60 km altitude and 30 km/s at 100 km altitude can be achieved. The three major limitations on performance are the maximum wall heat flux that can be removed by the cooling water, the maximum current that can be maintained without electrode erosion and subsequent stream contamination, and the maximum voltage gradient that can be maintained without destructive arc-over.

Measurements of constricted-arc performance show that such devices can simulate heat-transfer rates of high velocity entry. Furthermore, performance can be significantly augmented by improved cooling techniques and electrode designs.

## INTRODUCTION

The electric-arc plasma wind tunnel is an example of a ground-based test facility developed to fulfill a need introduced by the space age to simulate atmospheric heating of entering space vehicles. Although arc plasma facilities have many shortcomings, they have the important advantage of maintaining realistic heat-transfer rates to laboratory-fixed models for long periods of time.

*Presented at 13th Annual Technical Meeting of Institute of Environmental Sciences, Washington, D. C., April 10-12, 1967.

Early arc plasma facilities produced a maximum total enthalpy of about $4 \times 10^7$ J/kg, a specific energy slightly in excess of that required for satellite entry simulation. Later, the prospect of atmospheric entry at parabolic or hyperbolic velocity demanded higher performance plasma facilities that could produce total enthalpies corresponding to flight at velocities of above 12 km/s. As a result of this need, the Ames Research Center developed a constricted-arc supersonic jet apparatus that can duplicate the specific energy of most entry trajectories of current interest.

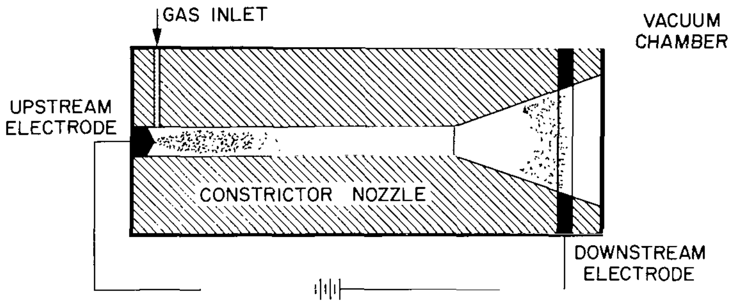

Figure 1.- Constricted-arc jet concept.

Constricted-arc supersonic jets are noteworthy because they can produce enthalpies about one order of magnitude higher than those produced by conventional plasma jets. The remarkable performance is due partly to the thermal constriction of the arc within a cooled tube of large length to diameter ratio. This concept, similar to that of the cascade arc studied by Maecker (ref. 1), is illustrated schematically in figure 1. A constricted-arc supersonic jet consists of a supersonic nozzle with electrodes at each end. A long, constant-area throat forms the arc constrictor tube. A continuous, direct-current arc is maintained concurrently with a longitudinal flow of air, or other gases from a pressurized reservoir. Positioning the downstream electrode in the supersonic portion of the nozzle permits the high enthalpies generated within the constrictor tube to be maintained as the heated air passes through the nozzle into the test section (ref. 2).

Although a constricted-arc jet duplicates certain aspects of atmospheric entry, such as total enthalpy and impact pressure for high altitudes, it does not produce a high-speed flow of cold air. The expansion of hot air through the nozzle is incomplete in the sense that a relatively hot stream is produced having an excess of excited species which move at reduced velocity. In spite of such difficulties, the constricted-arc jet has proved to be a useful research tool for heat-transfer studies at hyperbolic velocities. In addition, the device has potential application as a means for promoting chemical reactions at high temperature. To date, constricted-arc jets have been utilized to study radiation from shock layers, both of gas and of ablation vapors, ablation properties of materials, burn-up characteristics of satellite bodies and artificial meteors (ref. 3), and ionization recombination rates of nitrogen.

The four constricted-arc supersonic jets built and tested (refs. 3-6) differ primarily in size. Figure 2 shows the Arc Heated Planetary Gas Wind Tunnel, which incorporates the latest and largest of the constricted-arc jets, the performance of which is the subject of this paper.

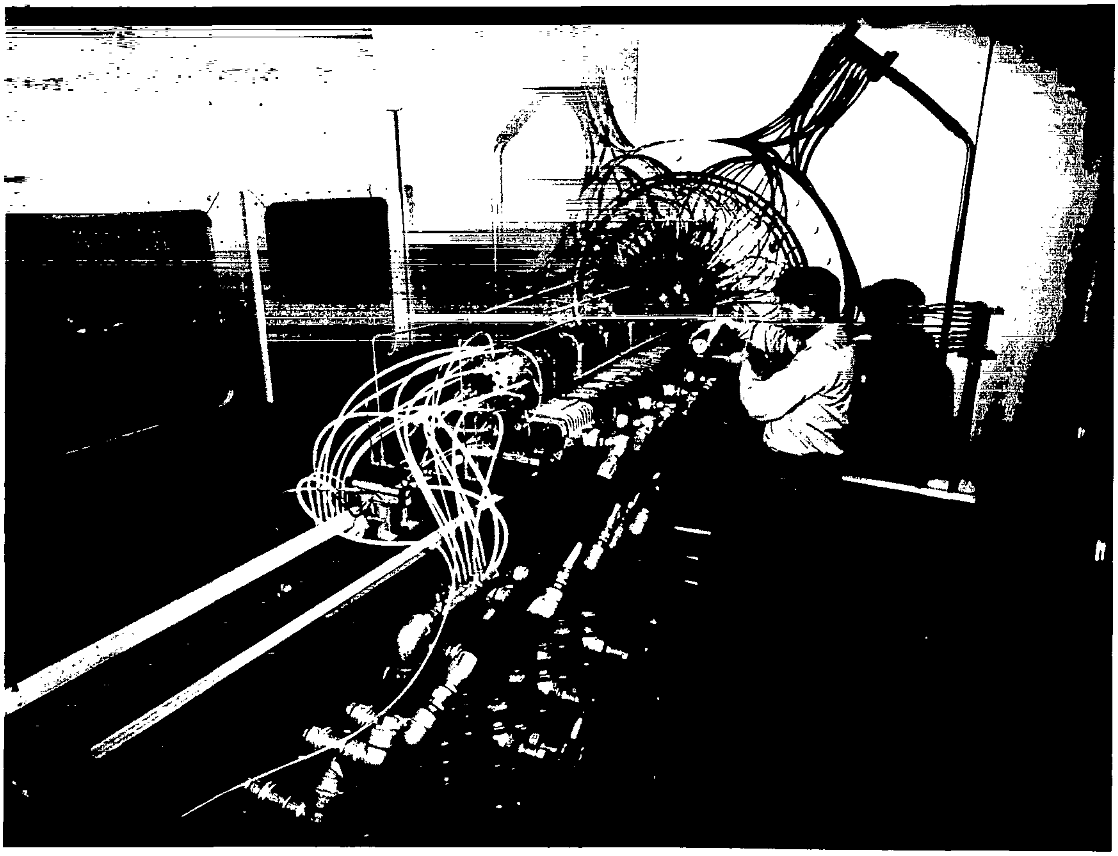

Figure 2.- Arc Heated Planetary Gas Wind Tunnel.

## SYMBOLS

| | |
|---|---|
| $A$ | nozzle area, $m^2$ |
| $C_H$ | coefficient of heating |
| $H$ | total enthalpy, J/kg |
| $I$ | arc current, A |
| $\dot{m}$ | gas flow rate, kg/s |
| $p_o$ | pressure at upstream end of constrictor tube, atmospheres |
| $p_{t,2}$ | impact pressure, $N/m^2$ |
| $q_{CONT}$ | stagnation-point heat-transfer rate for continuum flow, $W/m^2$ |
| $q_{FM}$ | stagnation-point heat-transfer rate for free molecular flow, $W/m^2$ |
| $q_t$ | stagnation-point heat-transfer rate, $W/m^2$ |

$q_w$ constrictor wall heat-transfer rate, W/m$^2$

R radius, m

u velocity, m/s

$\rho$ gas density, kg/m$^3$

Subscripts

AV mass average

CALC calculated

℄ center line

EXIT nozzle exit

MEAS experimentally determined

Superscript

* nozzle throat

APPARATUS

The plasma generator of the Arc Heated Planetary Gas Wind Tunnel is shown schematically in figure 3. With regard to construction details, the 2.54 cm internal diameter constrictor tube is 1.4 m long and is composed of 135 water-cooled rings. The rings are electrically insulated from each other by 1.8-mm-thick boron nitride washers, and are grouped into six modules to facilitate servicing. Air from a high-pressure gas storage system is introduced between constrictor rings in the first two modules. The supersonic portion of the nozzle also consists of a number of water-cooled rings that are insulated by 2.5-mm-thick boron nitride washers. The flow is expanded to a nozzle exit diameter of 0.46 m by the 30° included angle nozzle. The nozzle exhausts into a 27 cubic meter vacuum box which is pumped to atmosphere by a large 5-stage steam-ejector vacuum system.

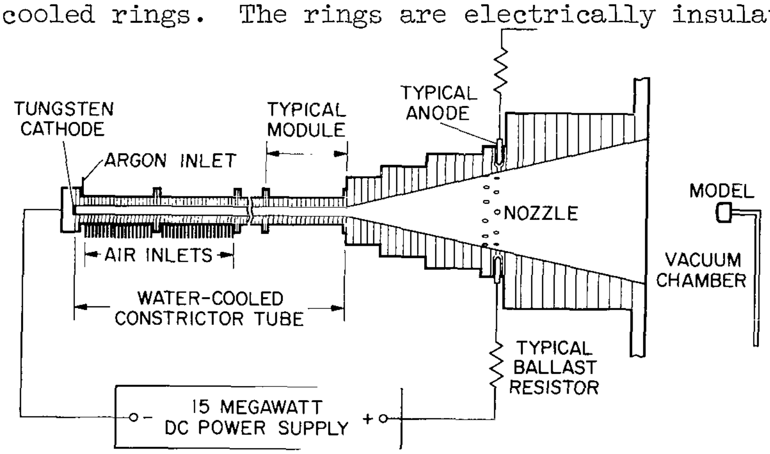

Figure 3.- Schematic drawing of Arc Heated Planetary Gas Wind Tunnel.

## CONSTRICTED-ARC JET PERFORMANCE

As discussed in appendix A, both total enthalpy and impact pressure must be known before convective heat transfer to a given blunt body in continuum flow can be specified. Similarly, total enthalpy and mass flux density specify heat-transfer rates in free-molecular flows, but mass flux density can be estimated from the impact pressure and total enthalpy. Therefore, total enthalpy and impact pressure can be regarded as the defining parameters for convective heat transfer in the stream of a constricted-arc jet, whether the flow be continuum or free molecular.

The simulation capabilities of the Arc Heated Planetary Gas Wind Tunnel (fig. 2) and of two smaller constricted-arc jets are shown in figure 4. This figure maps the regions of total enthalpy and impact pressure on the jet axes where operation has been demonstrated. Also included on the figure are lines of constant equivalent flight velocity, defined as the square root of twice the center-line total enthalpy, and lines of constant altitude, as obtained from the equivalent density $p_{t,2}/2H_{\text{℄}}$.

Figure 4 indicates that the Arc Heated Planetary Gas Wind Tunnel can simulate flight velocities up to 30 km/s at an altitude of about 100 km. At an equivalent velocity of 10 km/s, an altitude of about 85 km can be simulated. Figure 4 further illustrates that lower altitudes can be simulated when the flow is expanded through a nozzle of lower area ratio. For example, with the area ratio 22 nozzle (ref. 6), flight can be simulated at altitudes down to 60 km, whereas with the area ratio 160 nozzle (ref. 5), flight can be simulated in the intermediate altitude range from about 75 to 90 km. In these latter cases, the test body diameters that can be accommodated are relatively small, of course.

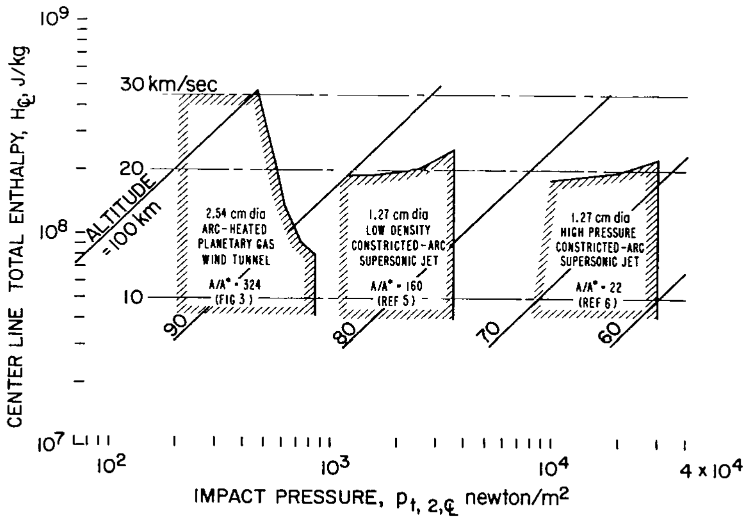


Figure 4.- Simulation capabilities of several constricted-arc jets.

## Enthalpy Determination

The local value of total enthalpy in the vicinity of a test body is required to describe the heat-transfer environment. The test bodies normally are mounted on the axes of constricted-arc jets and therefore are exposed to center-line total enthalpy. Unfortunately, an enthalpy probe that could operate at the low densities and high heat-transfer characteristic of the Arc Heated Planetary Gas Wind Tunnel was not available for the performance tests. For this reason the center-line total enthalpy is inferred from a combination of experimental measurements and theoretical calculations. A mass-average total enthalpy derived from experiment is multiplied by a calculated ratio of center line to average enthalpy to obtain the center-line total enthalpy.

The mass-average total enthalpy is defined as the quotient of the net power accepted by the gas and the flow rate. It is a measure of gross arc jet performance. Because the constricted-arc jet is water-cooled, one can measure the net power by subtracting the power absorbed by the cooling water from the electrical power supplied to the arc.

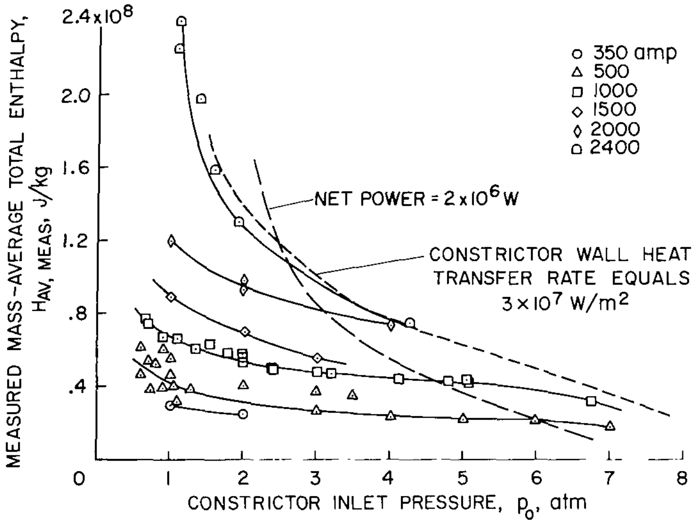


Figure 5.- Experimentally determined mass-average total enthalpy as a function of constrictor inlet pressure for various arc currents.

It is worthwhile to examine the mass-average total enthalpy capabilities of the Arc Heated Planetary Gas Wind Tunnel. Figure 5 shows the experimentally determined mass-average total enthalpy for various arc currents as a function of the pressure at the constrictor-tube inlet. It should be noted that increasing the air mass flow rate raises the pressure at fixed current. Thus, the figure can also be regarded as a plot showing variation of mass-average enthalpy at fixed current with mass flow rate.

The effect of inlet, or chamber, pressure on mass-average enthalpy is readily apparent from figure 5. Mass-average total enthalpy decreases with increasing pressure for a given current. This trend is due in part to radiation power loss to the constrictor wall, because radiation increases strongly with chamber pressure. As a result, the net power increases at a slower rate than the gas flow rate as pressure is increased at a constant current and, consequently, the mass-average total enthalpy decreases. At pressures below about 1 atmosphere, radiation is relatively unimportant as a heat loss mechanism, and as a result, enthalpies in excess of $2.5 \times 10^8$ J/kg can be achieved. At 7 atmospheres pressure, however, the maximum mass-average total enthalpy that has been reached to date is only $3.5 \times 10^7$ J/kg.

Although the mass-average enthalpy increases with increasing current, operational limits that restrict achievable enthalpy are eventually reached.

One of these is the maximum current that the electrodes can carry. The other is the heat-transfer rate that can be accommodated by the constrictor wall. A curve corresponding to a constrictor wall heat-transfer rate of $3 \times 10^7$ is shown in figure 5. This heat-transfer rate provides an adequate safety factor for state-of-the-art cooling, but does not set an absolute limit on the maximum enthalpy that can be achieved. A curve showing mass-average total enthalpies and corresponding constrictor inlet pressures for a net input of 2 MW is also shown in figure 5.

In a constricted-arc jet, the mass-average enthalpy is lower than the enthalpy on the jet axis. To indicate the differences between them, Watson calculated the ratio of center line to mass-average total enthalpy using numerical methods (ref. 7). Although the calculated center line to mass-average enthalpy ratio has not been directly verified by experiment, it is pointed out in appendix B that computed and measured mass-average total enthalpies generally agree well, suggesting that the calculated ratio is correct.

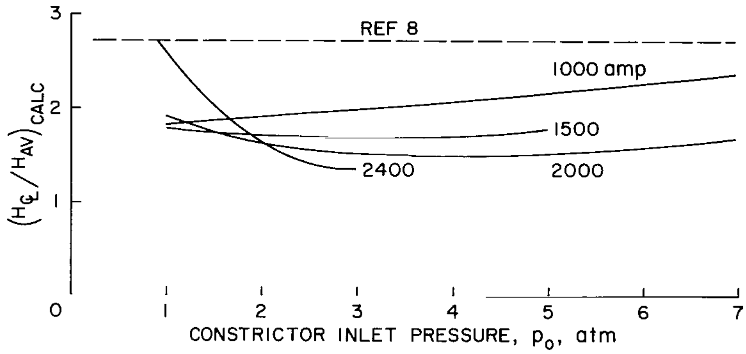


Figure 6.- Calculated center line to mass-average enthalpy ratio as a function of constrictor inlet pressure for various arc currents.

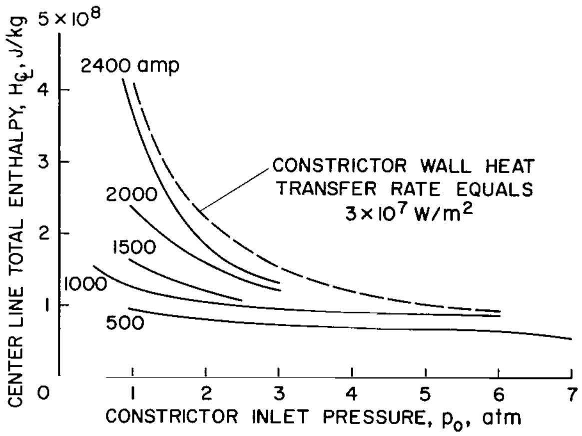


Figure 7.- Center-line total enthalpy versus constrictor inlet pressure for various arc currents.

Curves showing the calculated ratio of center line to mass-average total enthalpy as a function of the constrictor inlet pressure for various values of current are presented in figure 6. The ratio is a function of both pressure and current and varies from about 1.6 at high inlet pressure and low current to about 2.8 at low pressure and high current. The value of the ratio of center line to average enthalpy from the analysis of Stine and Watson (ref. 8) is also shown for comparison.

The center-line total enthalpy, the product of the measured mass-average total enthalpy (fig. 5) and the calculated ratio of center line to mass-average total enthalpy (fig. 6), is presented in figure 7 as a function of the constrictor inlet pressure for various values of current. The curve that corresponds to a constrictor wall heat-transfer rate of $3 \times 10^7$ W/m$^2$ is also shown. The trends with pressure and current are similar to those of the mass-average enthalpy deduced from measurements. Center-line total enthalpies in excess of $4 \times 10^8$ J/kg can be generated provided the constrictor inlet pressure is less than 1 atmosphere at a constrictor wall heat-transfer rate of $3 \times 10^7$ W/m$^2$. At 7 atmospheres, however, the center-line enthalpy at this wall heat-transfer rate is only about $8 \times 10^7$ J/kg.

## Impact Pressure Determination

Impact pressure is measured by a water-cooled probe in a straightforward manner. One precaution that is observed, however, is to electrically insulate the probe from the arc jet and the surrounding vacuum box to minimize disturbance to the electrically conductive stream. In a free-jet flow such as the test volume of the Arc-Heated Planetary Gas Wind Tunnel, the measured impact pressure varies considerably with streamwise location of the probe unless the static pressure at the nozzle exit is carefully matched to the vacuum box pressure. Because means were unavailable for balancing pressures, unique variations of impact pressure with constrictor inlet pressure at fixed current occur only at fixed probe locations in the test volume.

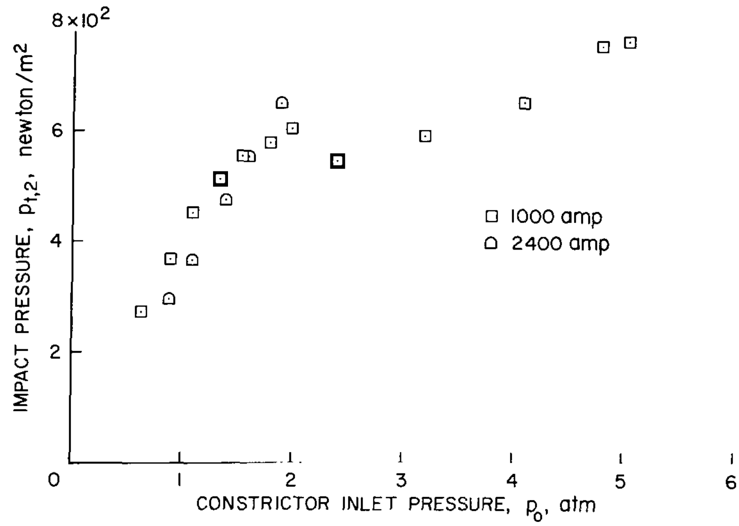


Figure 8.- Impact pressure as a function of constrictor inlet pressure for two arc currents.

Figure 8 shows impact pressure at a station 0.5 m downstream of the nozzle exit plane as a function of the pressure at the constrictor inlet for a range of currents from 1000 A to 2400 A. The data suggest that impact pressure is insensitive to an increase in arc current of a factor of 2. Impact pressure, however, increases systematically with constrictor inlet pressure at fixed current, but not in the linear manner that is characteristic of isentropic flows in supersonic nozzles.

## Stagnation-Point Heat-Transfer Rate

Given impact pressure and enthalpy, the stagnation-point heat-transfer rate for a blunt body can be calculated by means of equations and techniques discussed in appendix A. Further calculations can relate stagnation-point heat-transfer rate to the arc-heater parameters, current and constrictor inlet pressure, taking due account of the fact that in general the flow in the Arc Heated Planetary Gas Wind Tunnel test stream lies neither in the free-molecular nor in the continuum domain. It is shown in appendix A, however, that stagnation-point heat-transfer rate for a 2 cm diameter body is that due to essentially free-molecule flow. Consequently, uncertainties in the values of $C_H$ and $\rho u$ needed for the calculations have a large effect on the computed heat-transfer rate. The computed effects of arc current and constrictor inlet pressure on stagnation-point heat-transfer rate are presented in figure 9 for

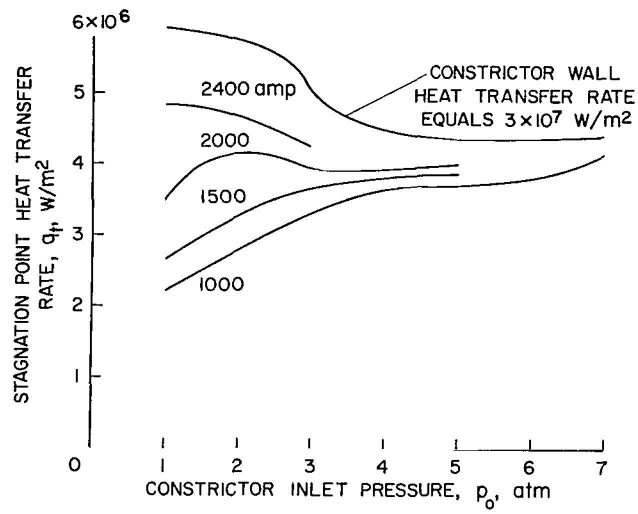


Figure 9.- Calculated stagnation-point heat-transfer rate for a 2-cm-diameter model as a function of constrictor inlet pressure.

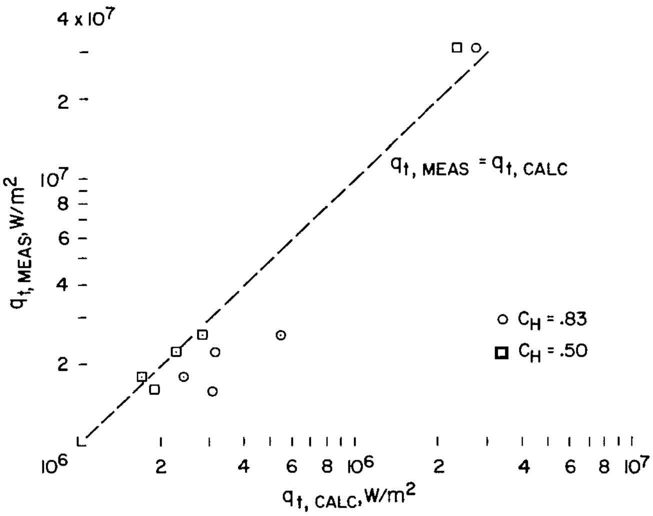


Figure 10.- Comparison of calculated and measured stagnation-point heat-transfer rate for a 2-cm-diameter calorimeter.

a 2 cm diameter nickel-plated copper calorimeter with a 1.15 cm nose radius. Stagnation-point heat-transfer rate calculated for the conditions of the tests increases with increasing arc current, but is relatively insensitive to constrictor pressure level. The stagnation-point heat-transfer rate corresponding to operation at $3\times10^7$ W/m² constrictor wall heat-transfer rate is also shown on figure 9. The curves suggest that a maximum stagnation-point heat-transfer rate of $6\times10^6$ W/m² can be achieved at a constrictor pressure of about 1 to 2 atmospheres.

A 1.15 cm nose-radius calorimeter was exposed to the test stream of the Arc Heated Planetary Gas Wind Tunnel to provide data for comparison with the calculated and stagnation-point heat-transfer rates. Figure 10 shows that when a heat-transfer coefficient, $C_H$, of 0.83 is selected, the predicted heat-transfer rates are lower than those measured. Good agreement was obtained, however, when a value $C_H = 0.5$ was selected.

The calorimeter was also exposed to the test stream of a 1.27 cm diameter constricted-arc supersonic jet (ref. 3). Because the density was about 20 times higher than that in the Arc Heated Planetary Gas Wind Tunnel, near-continuum flow conditions prevailed, so that the correction for free-molecular effects was small. Again, the measured and calculated heat-transfer rates are compared in figure 10. Because good agreement is demonstrated at the relatively high density where effects of uncertainties in $C_H$ and $\rho u$ are small, it is concluded that the center-line total enthalpies estimated from figure 4 are not in serious error.

## Radial Impact Pressure and Heat-Transfer Rate Profiles

The constrictor-tube radial flow profiles, calculated as described in appendix B, suggest that the test-section flow profiles would be nonuniform. Measured distributions of impact pressure and stagnation-point heat-transfer

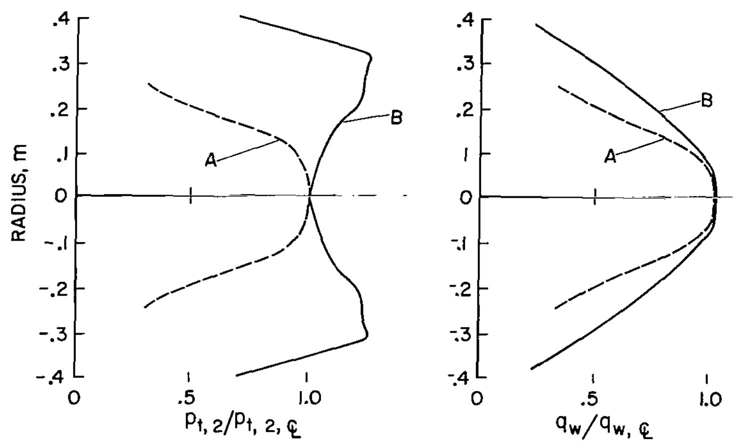


Figure 11.- Measured normalized radial profiles of impact pressure and stagnation-point heat-transfer rate.

rate across the test section confirm this hypothesis, as shown in figure 11. Normalized stagnation-point heat-transfer rate and impact pressure are plotted as a function of radial distance for two operating conditions of the Arc Heated Planetary Gas Wind Tunnel. For condition A, the center-line total enthalpy is about $10^8$ J/kg and the center-line impact pressure is about 400 N/m$^2$. Condition B represents a higher density operating point where the center-line total enthalpy is $5\times10^7$ and the center-line impact pressure is 600 N/m$^2$. The profiles (fig. 11) suggest that although operating conditions can be adjusted to produce a relatively uniform radial profile of impact pressure, the heat-transfer rate will be distributed nonuniformly regardless of current or constrictor inlet pressure. Consequently, heat-transfer tests should preferably use an axisymmetric body with its axis coincident with the jet center line. Relatively large bodies can be tested if the above restrictions are observed, because the stream tube that supplies the fluid to the stagnation point has a smaller diameter than the body. For example, the heating-rate distribution over the model remains unchanged with models as large as 1/3 the nozzle exit diameter.

## LIMITS ON MAXIMUM ENTHALPY

The current or the pressure levels or both that can be achieved in constricted-arc apparatus are limited by: the maximum current which the electrodes can carry; the maximum voltage drop which can be maintained between adjacent rings without destructive arc-over; and, as was mentioned previously, the maximum heat-transfer rate that the constrictor wall can accommodate. With regard to electrode failure, it is known that current carried by a tungsten cathode decreases with increasing pressure. Although the thoriated tungsten button cathode is adequate for currents up to 2400 A and pressures up to 7 atm, future operations will require an upgrading of the cathode. Experiments with tungsten additives other than thoria promise cathodes that operate at pressures two or three times higher than can be achieved at present. The behavior of barium-calcium-aluminate as an additive (ref. 9) is especially noteworthy. Current capacities of tungsten cathodes with additives either of barium-calcium-aluminate or of thoria were compared at various pressures in a nitrogen atmosphere. Figure 12 shows maximum permissible current as a function of pressure that tungsten cathodes could carry, and demonstrates that the barium-calcium-aluminate additive improves performance appreciably.

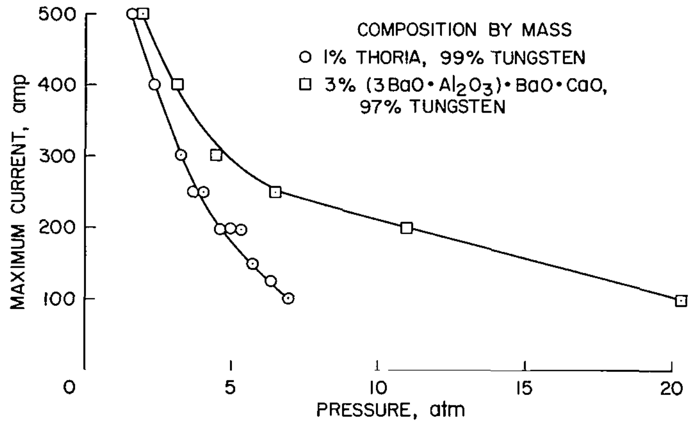

Figure 12.- Maximum current as a function of pressure for 1.3-cm-diameter thoria-tungsten and barium calcium aluminate-tungsten cathodes in nitrogen.

The most frequent and least understood failure is electric arc-over between adjacent constrictor rings during operation at high pressure associated with high flow rate. All or part of the current flows from one constrictor ring to the next adjacent to the wall with subsequent removal of ring material and eventual failure. This phenomenon, an insulation failure, would be expected to be a direct function of the voltage drop between adjacent rings but it appears also to be a function of the symmetry of flow injection. For example, at the upstream, or cathode, end of the constrictor tube where the flow is normally injected, a voltage difference of 30 to 40 V between adjacent rings may lead to serious voltage breakdown problems, but at the downstream end of the constrictor, where axial symmetry prevails, differences up to 70 V between adjacent rings may exist without arc-over. When high flow rates are required, the local voltage gradient is controlled by the introduction of flow gradually along the upstream portion of constrictor tube in such a manner that the voltage difference between adjacent rings never exceeds 40 V.

The Arc Heated Planetary Gas Wind Tunnel has been successfully operated at an overall voltage of 5.6 kV; the corresponding pressure was 7 atm and the current was 500 A.

With regard to the limit imposed by constrictor wall heat transfer, the maximum rate at which the cooling water can remove heat from the constrictor tube involves a number of factors such as the thickness and thermal conductivity of the wall, the shape and radius of curvature of the coolant passage, the water pressure and velocity, and the amount of scale that has collected in the cooling passages. In addition the mechanical resistance of the constrictor ring to the combined effects of thermal and hydraulic stresses also must be considered, for, in practice, "burn-out" cooling failures rarely occur within the water-cooled parts of constricted-arc jets. Instead, water leaks from brazed or welded seams which open after repeated arc starts and stops characterize operation at high constrictor heat-transfer rates. Such failures depend on the past history of arc jet operation and are not generally predictable. Nevertheless, better cooling can minimize joint fatigue failures by reducing the constrictor ring temperature for a given heat-transfer rate, or permit operation at high enthalpies without increasing the failure rate.

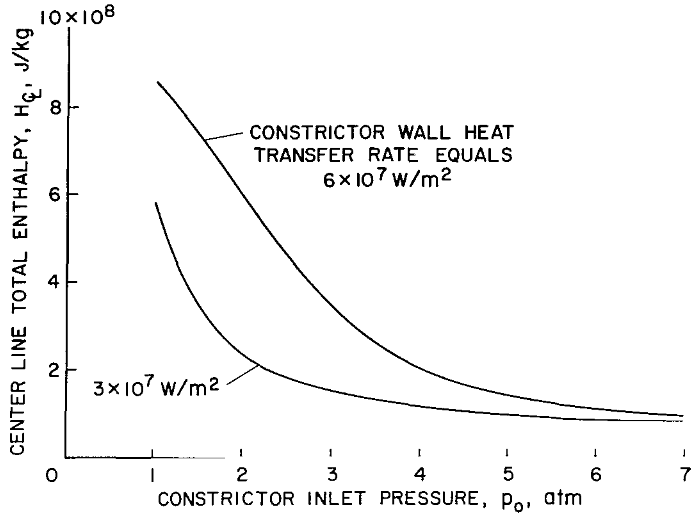


Figure 13.- Calculated center-line total enthalpy for two values of constrictor wall heat-transfer rate.

The effect on enthalpy of operating at two different levels of wall heat-transfer rate is illustrated in figure 13. Center-line total enthalpy has been calculated as a function of constrictor inlet pressure for constrictor-wall heat-transfer rates of $3\times10^7$ and $6\times10^7$ W/m$^2$. The effect on enthalpy of doubling the wall heat-transfer rate is seen to be small at 7 atm where a 15 percent increase in total enthalpy was calculated. The gain in enthalpy increases for decreasing pressure and, at 3 atm or less, the center-line total enthalpy is approximately doubled when the wall heat-transfer rate is doubled.

## CONCLUSIONS

A series of constricted-arc jets have been shown to produce remarkably high enthalpies. The performance and simulation capabilities of the latest of these, the Arc Heated Planetary Gas Wind Tunnel, has been determined by various measurements and by numerical analysis and prompts the following conclusions.

The maximum mass-average total enthalpy which was achieved exceeded $2.5\times10^8$ J/kg at atmospheric pressure. The mass-average total enthalpy decreased with increasing pressure to $3.5\times10^7$ J/kg at 7 atm. High power inputs to the air stream were also obtained. Over 2 MW could be delivered to the air stream for a range of constrictor inlet pressures of from 2 to 7 atm.

The center-line total enthalpy was estimated from the product of the measured mass-average total enthalpy and a calculated ratio of center line to mass-average enthalpy. The maximum value exceeded $4\times10^8$ J/kg at atmospheric pressure and $8\times10^7$ J/kg at 7 atm. Consideration of the attainable ranges of center-line total enthalpy and impact pressure, which are important heat-transfer parameters, indicates that heat-transfer tests can be made at simulated velocities up to 30 km/s at 100 km simulated altitude. At 85 km simulated altitude, heat-transfer rates corresponding to flight at 10 km/s can be duplicated.

The flow in the test section of the Arc Heated Planetary Gas Wind Tunnel was neither free molecular nor continuum. Accordingly, stagnation-point heat-transfer rate was calculated for the transitional flow domain. The calculated rates were found to be somewhat lower than the corresponding measured values and the difference between them was believed to be due to uncertainties in the heat-transfer coefficient.

The performance reported in this paper was limited by occasional constrictor ring arc-over and by water leaks associated with high constrictor wall heat-transfer rate operation. Better flow injection and more efficient constrictor ring cooling techniques will improve the arc jet performance by increasing the permissible air flow rate and constrictor wall heat-transfer rate.

Measured radial profiles of impact pressure and stagnation-point heat-transfer rate were found to be nonuniform as was predicted by the numerical solutions. In spite of the nonuniform radial flow profiles, useful tests at very high enthalpy have been conducted in the Arc Heated Planetary Gas Wind Tunnel.

Ames Research Center
National Aeronautics and Space Administration
Moffett Field, Calif., 94035, April 10, 1967
129-02-08-02-00-21

## APPENDIX A

## STAGNATION-POINT HEAT-TRANSFER RATE CALCULATIONS

The calculation of stagnation-point convective heat-transfer rate for blunt bodies in the test stream of constricted-arc jets is by no means straightforward. The usual heat-transfer-rate equations have been developed for a much lower range of enthalpies. Furthermore, the high enthalpies result in low densities and the flow for the apparatus of figure 3 is transitional. However, it is still useful to make the calculations and to compare them with calorimeter measurements.

Because the flow for the Arc Heated Planetary Gas Wind Tunnel is neither entirely free molecular nor continuum, an interpolation technique between the two extremes is necessary. The bridging equation of reference 10 provides a convenient method of estimating the heat-transfer rate. Both free molecular and continuum heat-transfer rates are calculated and applied to the following equation:

$$q_t = q_{CONT}[1 - \exp(-q_{FM}/q_{CONT})] \qquad (A1)$$

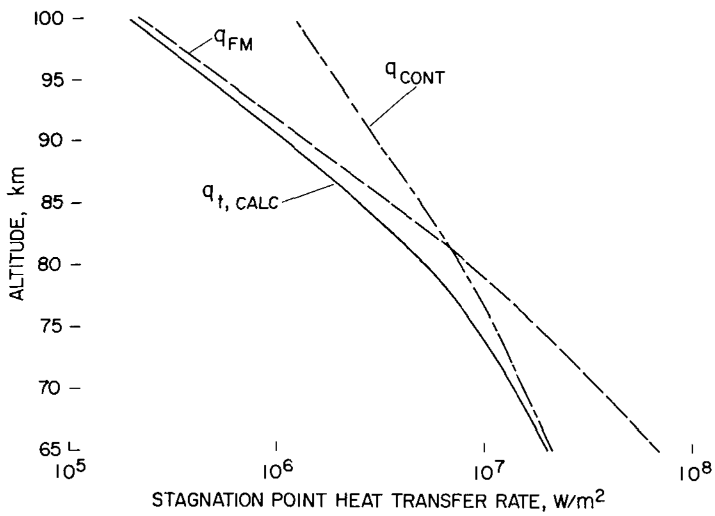


Figure 14.- Typical variation of stagnation-point heat-transfer rate with altitude for a 2-cm-diameter model at 10 km/s.

The bridging equation favors the lower of the two heat-transfer rates, as is illustrated in figure 14, where the free molecular, continuum, and resultant heat-transfer rates for a 2 cm diameter body are plotted as a function of altitude for a velocity of 10 km/s. At an altitude of 100 km the heat-transfer rate approaches the free molecular value, and at an altitude of 65 km the heat-transfer rate is nearly equal to the value calculated for continuum flow.

In the calculation of heat-transfer rate for the calorimeters, the stagnation-point pressure, $p_{t,2}$, the total enthalpy at the jet center line and the nose radius are known. The calorimeter heat-transfer rate is calculated as follows:

$$q_{CONT} = 3.7\times10^{-5}(p_{t,2}/R)^{1/2}H_{\mathrm{CL}}^{0.995} , \quad \mathrm{W/m^2} \qquad (A2)$$

from reference 11, and

$$q_{FM} = C_H \rho u H_{\mathbb{C}} , \qquad W/m^2 \tag{A3}$$

in mks units.

The calculation of $q_{FM}$ was complicated because measured values of $\rho u$ were not available. The best method of estimating $\rho u$ is to assume that $p_{t,2}$ is equal to $\rho u^2$. Then $\rho u$ is given by $p_{t,2}/u$, where $u$ can be estimated from the total enthalpy and the nozzle expansion area ratio, $A_{EXIT}/A^*$.

$$\rho u = p_{t,2}/(2H_{\mathbb{C}})^{1/2}[H_{\mathbb{C}}/(1/2)u^2]^{1/2} , \qquad kgm^{-2}\ s^{-1} \tag{A4}$$

where $H_{\mathbb{C}}/(1/2)u^2$ is the ratio of total to kinetic energy. This ratio is about 2.0 for the nozzle of figure 3, based on nozzle calculations of reference 12, and scattered velocity measurements.

The value of $C_H$ is also uncertain. Published accommodation coefficients for cold, diatomic nitrogen and oxygen on a nickel surface are given as 0.824 and 0.862, respectively (ref. 13). A value of 0.83 was deduced for air from the above values; however, the actual test gas is highly dissociated and ionized so that the actual coefficient of heating may be much different.

## APPENDIX B

## CONSTRICTED-ARC ANALYSIS

In the constricted-arc supersonic jet, the losses occurring within the nozzle are approximately nullified by the concurrent ohmic heating. As a result, the enthalpy at the downstream end of the constrictor, where the enthalpy can be calculated, is comparable to that of the nozzle exit where the heat-transfer tests are conducted.

The mathematical analyses of the heating process within the constrictor tube have been very useful to the designer of constricted-arc jets. For example, the Stine-Watson analysis (ref. 8) assisted the development of the constricted-arc jets by providing an approximate description of the heat addition and loss mechanisms, and by defining important design parameters. However, it neglected radiation which, as mentioned before, is an important loss mechanism at pressures above 2 atmospheres. Consequently, a method of analysis developed by Watson (ref. 7) was used.

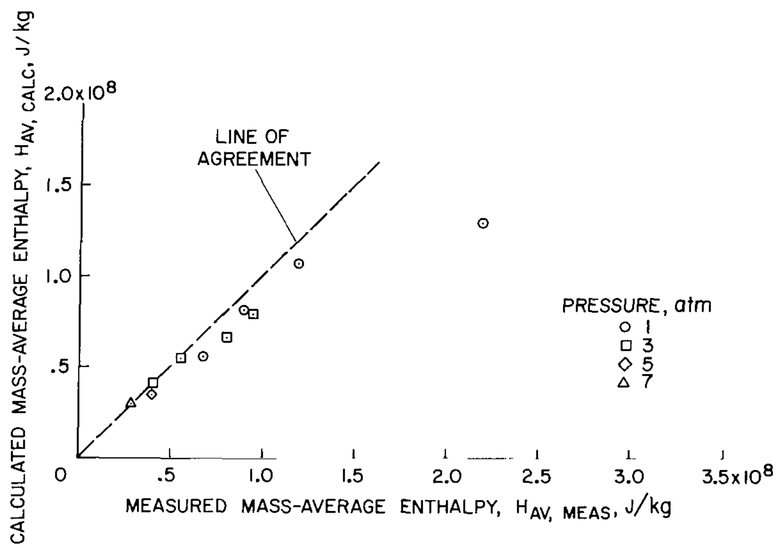


Figure 15. Comparison of calculated and experimentally determined mass-average total enthalpy.

Watson's method, programmed for the IBM 7094 computer, includes radiation, nonuniform gas mass flux density, viscosity, flow turbulence and real gas properties. The results obtained from this theoretical approach agree favorably with experiment whenever comparison has been made. For example, figure 15 compares the calculated and experimentally determined mass-average total enthalpy. Good agreement exists over a wide range of pressures and enthalpies.

The computer analysis can also provide a better understanding of how the constricted-arc jets operate. For example, enthalpy generation can be studied. But in order to study the build-up of enthalpy within the constrictor tube, it is first necessary to examine the mass flux density. Figure 16(a) presents a number of computer-generated radial profiles of mass flux density at various axial locations along the constrictor tube for a typical operating point. Notice that the gas is initially forced to the constrictor wall by the arc, depleting the mass flux density at the tube center line. Further downstream the gas begins to enter the core and if the tube is long enough, the mass flux density will become approximately uniform as shown in the last profile.

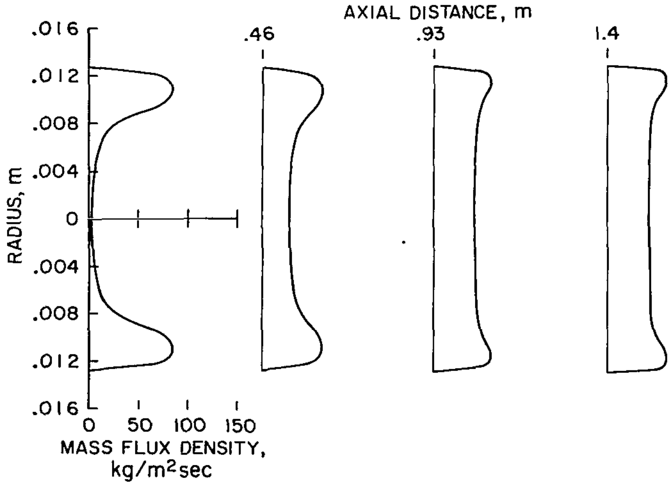


(a) Mass flux density.

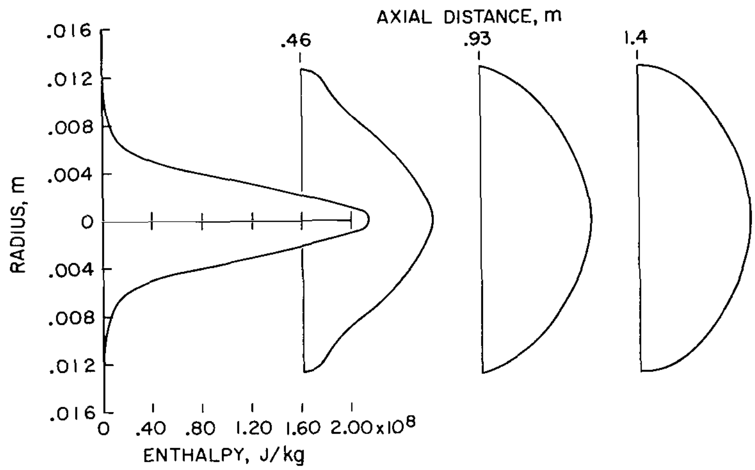


(b) Enthalpy.

Figure 16.- Typical calculated constrictor radial flow profiles at various axial locations.

The corresponding radial enthalpy profiles are presented in figure 16(b). Near the upstream end of the constrictor tube, the enthalpy rises to a very high value in the rarefied flow. Downstream the core is cooled by the incoming air and the center-line enthalpy decreases and remains relatively constant thereafter. The enthalpy profiles become broader at increasing axial distance as energy is added to the airstream, but because the process is not adiabatic, the enthalpy profiles are always peaked at the jet center line. These constrictor profiles suggest that the test-section profiles will also be nonuniform.

## REFERENCES

1. Maecker, H.: Messung und Auswertung von Bogencharakteristiken (Ar, $N_2$). Zeitschrift fur Physik, vol. 158, 1960, pp. 392-404.

2. Stine, H. A.: The Hyperthermal Supersonic Aerodynamic Tunnel. NASA Proc. International Symposium on High Temperature Technology, Sept. 1963, Butterworth, Wash., 1964.

3. Shepard, C. E.; Vorreiter, J. W.; Stine, H. A.; and Winovich, W.: A Study of Artificial Meteors as Ablators. NASA TN D-3740, 1967.

4. Shepard, C. E.; Watson, V. R.; and Stine, H. A.: Evaluation of a Constricted-Arc Supersonic Jet. NASA TN D-2066, 1964.

5. Vorreiter, J. W.; and Shepard, C. E.: Performance Characteristics of the Constricted-Arc Supersonic Jet. Proc. 1965 Heat Transfer and Fluid Mechanics Institute, June 1965, pp. 42-49.

6. Park, C.; and Okuno, A. F.: Diagnosis of High-Density, Highly Ionized Nitrogen Wind Tunnel Flows. Proc. 2nd International Congress on Instrumentation in Aerospace Simulation Facilities, Stanford Univ., Aug. 29-31, 1966.

7. Watson, V. R.: Comparison of Detailed Numerical Solutions with Simplified Theories for the Characteristics of the Constricted-Arc Plasma Generator. Proc. 1965 Heat Transfer and Fluid Mechanics Institute, June 1965, pp. 24-41.

8. Stine, H. A.; and Watson, V. R.: The Theoretical Enthalpy Distribution of Air in Steady Flow Along the Axis of a Direct-Current Electric Arc. NASA TN D-1331, 1962.

9. Bade, W.; and Yos, J.: Theoretical and Experimental Investigation of Arc Plasma Generation Technology. Part II, vol. I, AVCO Rep. RAD-TR-63-11, 1964.

10. Matting, F. W.; and Chapman, D. R.: Analysis of Surface Ablation of Noncharring Materials with Description of Associated Computing Program. NASA TN D-3758, 1966.

11. Marvin, J. G.; and Deiwert, G. S.: Convective Heat Transfer in Planetary Gases. NASA TR R-224, 1965.

12. Yoshikawa, K. K.; and Katzen, E. D.: Charts for Air-Flow Properties in Equilibrium and Frozen Flows in Hypervelocity Nozzles. NASA TN D-693, 1961.

13. Admur, I.; and Guildner, L. A.: Thermal Accommodation Coefficients on Gas-Covered Tungsten, Nickel, and Platinum. J. Am. Chem. Soc., vol. 79, 1957, p. 311.



NASA-Langley, 1968 — 21 A-2632

NATIONAL AERONAUTICS AND SPACE ADMINISTRATION
WASHINGTON, D. C. 20546

OFFICIAL BUSINESS

**FIRST CLASS MAIL**

POSTAGE AND FEES PAID
NATIONAL AERONAUTICS AND
SPACE ADMINISTRATION

CIL 001 50 51 3DS 68134 00903
AIR FORCE WEAPONS LABORATORY/AFWL/
KIRTLAND AIR FORCE BASE, NEW MEXICO 8711

ATT MISS MADELINE F. CANOVA, CHIEF TECHN
LIBRARY /WLIL/

If Undeliverable (Section 158 Postal Manual) Do Not Return

*"The aeronautical and space activities of the United States shall be conducted so as to contribute . . . to the expansion of human knowledge of phenomena in the atmosphere and space. The Administration shall provide for the widest practicable and appropriate dissemination of information concerning its activities and the results thereof."*

—NATIONAL AERONAUTICS AND SPACE ACT OF 1958

# NASA SCIENTIFIC AND TECHNICAL PUBLICATIONS

TECHNICAL REPORTS: Scientific and technical information considered important, complete, and a lasting contribution to existing knowledge.

TECHNICAL NOTES: Information less broad in scope but nevertheless of importance as a contribution to existing knowledge.

TECHNICAL MEMORANDUMS: Information receiving limited distribution because of preliminary data, security classification, or other reasons.

CONTRACTOR REPORTS: Scientific and technical information generated under a NASA contract or grant and considered an important contribution to existing knowledge.

TECHNICAL TRANSLATIONS: Information published in a foreign language considered to merit NASA distribution in English.

SPECIAL PUBLICATIONS: Information derived from or of value to NASA activities. Publications include conference proceedings, monographs, data compilations, handbooks, sourcebooks, and special bibliographies.

TECHNOLOGY UTILIZATION PUBLICATIONS: Information on technology used by NASA that may be of particular interest in commercial and other non-aerospace applications. Publications include Tech Briefs, Technology Utilization Reports and Notes, and Technology Surveys.

*Details on the availability of these publications may be obtained from:*

**SCIENTIFIC AND TECHNICAL INFORMATION DIVISION**

**NATIONAL AERONAUTICS AND SPACE ADMINISTRATION**

**Washington, D.C. 20546**